AFRL-RH-FS-TR-2017-0017

Effects of Variable Spot Size on Human Exposure to 95-GHz Millimeter Wave Energy

James E. Parker
Eric J. Nelson
Charles W. Beason

General Dynamics Information Technology

Michael C. Cook

Bioeffects Division
Radio Frequency Bioeffects Branch

May 2017

Air Force Research Laboratory
711th Human Performance Wing
Airman Systems Directorate
Bioeffects Division
Radio Frequency Bioeffects Branch
4141 Petroleum Road
JBSA Fort Sam Houston, Texas 78234-2644

NOTICE AND SIGNATURE PAGE

Using Government drawings, specifications, or other data included in this document for any purpose other than Government procurement does not in any way obligate the U.S. Government. The fact that the Government formulated or supplied the drawings, specifications, or other data does not license the holder or any other person or corporation; or convey any rights or permission to manufacture, use, or sell any patented invention that may relate to them.

This report was cleared for public release by the 88th ABW Public Affairs Office and is available to the general public, including foreign nationals. Copies may be obtained from the Defense Technical Information Center (DTIC) (http://www.dtic.mil).

"Effects of Variable Spot Size on Human Exposure to 95-GHz Millimeter Wave Energy"

(AFRL-RH-FS-TR- 2017 - 0017) has been reviewed and is approved for publication in accordance with assigned distribution statement.

JOHNSON.LELAND.R.1161902612

Digitally signed by JOHNSON.LELAND.R.1161902612
DN: c=US, o=U.S. Government, ou=DoD, ou=PKI, ou=USAF, cn=JOHNSON.LELAND.R.1161902612
Date: 2017.06.05 06:41:11 -05'00'

LELAND JOHNSON, DR-III, DAF
Contract Monitor
Radio Frequency Bioeffects Branch

MILLER.STEPHANIE.A.1230536283

Digitally signed by MILLER.STEPHANIE.A.1230536283
DN: c=US, o=U.S. Government, ou=DoD, ou=PKI, ou=USAF, cn=MILLER.STEPHANIE.A.1230536283
Date: 2017.08.07 09:26:25 -05'00'

STEPHANIE A. MILLER, DRIV, DAF
Chief, Bioeffects Division
Airman Systems Directorate
711th Human Performance Wing
Air Force Research Laboratory

This report is published in the interest of scientific and technical information exchange, and its publication does not constitute the Government’s approval or disapproval of its ideas or findings.

REPORT DOCUMENTATION PAGE

Form Approved
OMB No. 0704-0188

1. REPORT DATE *(DD-MM-YYYY)*	**2. REPORT TYPE**	**3. DATES COVERED** *(From – To)*
11-05-2017	Interim	December 2006 – May 2017

4. TITLE AND SUBTITLE

Effects of Variable Spot Size on Human Exposure to 95-GHz Millimeter Wave Energy

5a. CONTRACT NUMBER
FA8650-13-D-6368-0007

5b. GRANT NUMBER
N/A

5c. PROGRAM ELEMENT NUMBER
62202F

6. AUTHOR(S)

James E. Parker, Eric J. Nelson, Charles W. Beason, and Michael C. Cook

5d. PROJECT NUMBER
N/A

5e. TASK NUMBER
N/A

5f. WORK UNIT NUMBER
HOEB

7. PERFORMING ORGANIZATION NAME(S) AND ADDRESS(ES)

General Dynamics Information Technology; Air Force Research Laboratory, 711th Human Performance Wing, Airman Systems Directorate, Bioeffects Division, Radio Frequency Bioeffects Branch (711 HPW/RHDR)
4141 Petroleum Road
JBSA Fort Sam Houston, Texas 78234-2644

8. PERFORMING ORGANIZATION REPORT NUMBER
N/A

9. SPONSORING / MONITORING AGENCY NAME(S) AND ADDRESS(ES)
Air Force Materiel Command, Air Force Research Laboratory,
711th Human Performance Wing, Airman Systems Directorate,
Bioeffects Division, Radio Frequency Bioeffects Branch
4141 Petroleum Road
JBSA Fort Sam Houston, Texas 78234-2644

10. SPONSOR/MONITOR'S ACRONYM(S)
711 HPW/RHDR

11. SPONSOR/MONITOR'S REPORT NUMBER(S)
AFRL-RH-FS-TR-2017-0017

12. DISTRIBUTION / AVAILABILITY STATEMENT
Distribution A: Approved for public release; distribution unlimited (P.A. Case No. TSRL-PA-2017-0191, 2 Aug 17).

13. SUPPLEMENTARY NOTES
This report was declassified by: ADT SCG, dated 9 Nov 2011; Declassified on 5 Sep 2013 (previously AFRL-RH-BR-TR-2011-0008)

14. ABSTRACT

The report documents two studies that were conducted to quantify human behavioral responses to 95-GHz millimeter wave (MMW) exposures employing differing beam sizes and power densities. Previously, the speed of the repel response was found to be dependent upon the power density and spot size on the target, but the exact form of this function was unclear. To provide clarity of the repel effect function, we investigated two experimental paradigms. Experiment 1 examined the repel times of stationary subjects at combinations of three MMW power densities and five spot sizes. Experiment 1 results confirmed that repel times decreased with increasing beam size, although the strength of this relationship varied with power density. Experiment 2 investigated the extent to which the Experiment 1 relationships between beam size and repel time could be extrapolated to moving subjects. Subjects were required to throw balls into a net while being targeted by the MMW beam. Results indicated similar performance at the four largest spot sizes tested, and better subject activity performance (i.e., decreased MMW effectiveness) at the smallest spot size.

15. SUBJECT TERMS Avoidance, behavior, millimeter waves, nonlethal weapons, radiofrequency

16. SECURITY CLASSIFICATION OF:			**17. LIMITATION OF ABSTRACT**	**18. NUMBER OF PAGES**	**19a. NAME OF RESPONSIBLE PERSON**
Unclassified					L. Johnson
a. REPORT	**b. ABSTRACT**	**c. THIS PAGE**			**19b. TELEPHONE NUMBER** *(include area code)*
Unclassified	Unclassified	Unclassified	U	31	N/A

Standard Form 298 (Rev. 8-98)
Prescribed by ANSI Std. Z39.18

THIS PAGE INTENTIONALLY LEFT BLANK

TABLE OF CONTENTS

LIST OF FIGURES

LIST OF TABLES

LIST OF ACRONYMS

711 HPW/RHDR	Air Force Research Laboratory, 711th Human Performance Wing, Airman Systems Directorate, Bioeffects Division, Radio Frequency Bioeffects Branch
ADS	Active Denial System
AFRL	Air Force Research Laboratory
CLT	Carbon-loaded Teflon
FWHM	Full width half maximum
IR	Infrared
MMW	Millimeter Wave
SG	Silent Guardian™
TTE	Time to effect

ACKNOWLEDGEMENTS

The authors gratefully acknowledge the following individuals for providing valuable technical, medical, and administrative expertise over the course of these studies: Ms. Stephanie A. Miller, Dr. Jeffrey N. Whitmore, Mr. David A. Fines, TSgt Suellen A. Hendrix, Capt James C. Belcher, Mr. Justin R. Vendola, Col Breck J. LeBegue, LtCol L. Michelle Bryce, Ms. Kalyn M. Yaws, Mr. Leland R. Johnson, Mr. Charles T. Kuhnel, Mr. Kevin S. Mylacraine, Mr. Francis A. Ruhr, Dr. Diana L. Loree, 1Lt Philip A. Amirault, Mr. William F. McCullough, Mr. Scott M. Orth, Mr. Paul R. Pelletier, Mr. Anthony E. Baros, and Mr. Kenneth M. Leeson, 1Lt Heather R. Rodriguez-Morris, 2Lt David R. Williams, Mr. Donicio Chama, Mr. James W. Staggs, Capt Adam Gubbels, Ms. Elizabeth L. Witherspoon, Ms. Lori A. Allen, Ms. Hilda D. Hall, Ms. Valinda M. Grimes, Ms. Melissa Tarango, Mr. Thomas E. DeAngelis, and Ms. M. Kathy Hitt.

EXECUTIVE SUMMARY

The present research was designed to quantify responses to 95-GHz millimeter wave (MMW) exposures employing beams of differing sizes (viz., two-dimensional full width, half maximum [FWHM] spots ranging from 0.46 to 2.07 m^2). Previous laboratory and field studies have indicated that the speed of the repel response is dependent upon, not only the power density on the target, but also the amount of the target surface area that is illuminated by the MMW beam. That is, given an initially stationary biological target, as more of the target area is illuminated by the beam, the quicker the initiation of the repel response becomes (i.e., the more quickly the target moves out of or away from the beam). However, the exact form of the function relating area illuminated to repel time is unclear. Two studies were conducted to better quantify this relationship. Experiment 1 examined the repel times of initially stationary human subjects in response to 95-GHz MMW exposures at each factorial combination of three power densities (where the power densities were among the following values 1.6, 1.85, 2.1, 2.4, 2.7, and 3.0 W/cm^2) and five spot sizes (where the two-dimensional FWHM elliptical spot area was 0.46, 0.62, 0.90, 1.40, and 2.07 m^2, and the eccentricity was 0.75). Experiment 1 results confirmed that repel times decreased with increasing beam diameter, although the strength of this relationship varied with power density. In general, at the higher power densities employed in this study (specifically, greater than 2.4 W/cm^2), the relationship between repel time and beam size becomes invariant for the spot sizes employed in this study.

Experiment 2 was designed to determine the degree to which the relationships between beam size and repel time established in Experiment 1 could be extrapolated to the case of applying an exposure energy to moving (non-stationary) subjects. In Experiment 2, subjects were required to throw balls into a net while being targeted by a 95-GHz MMW beam. Exposures were conducted employing the same five beam sizes used in Experiment 1, where the MMW transmitter operator was free to engage the subject as many times as possible during the event. Effectiveness was measured as the difference between a subject's performance during "actual" exposures when they were targeted by the 95-GHz system and that same subject's performance during "sham" exposures (i.e., when they were not targeted). Results indicated that the system was less effective at the smallest of the five beam sizes (0.46 m^2).

1.0 INTRODUCTION

Millimeter waves (MMWs), specifically those at the 95-GHz frequency, have been employed as the basis of an anti-personnel, non-lethal weapon system known as the Active Denial System (ADS). This system uses advanced technology to provide a non-lethal capability, which has a range greater than that of small arms fire, by directing a focused beam of MMWs, traveling at the speed of light, toward the designated biological target. Once the beam reaches the target, MMW energy penetrates the skin to a depth of approximately 0.3 mm (Erwin & Hurt, 1981; Gandhi & Riazi, 1986), resulting in rapid skin heating and an accompanying sensation of intolerable heating that causes reflexive movement away from the beam. The sensation immediately ceases when the individual moves out of the beam or when the system's operator turns the beam off. ADS has a very low risk of injury because the target's reflexive response causes movement out of the beam before skin heating can reach levels likely to cause thermal damage. In fact, over a decade of research has demonstrated that the desired behavioral response (i.e., rapid escape/repel) can be readily produced at energy levels well below those which cause burns in animals and humans. Of the more than 10,000 exposures that have occurred to date under human-use protocols, only minor injuries (consisting of blistering at the exposure site) have been observed (at a rate of approximately 0.1%).

The present research was designed to quantify responses to 95-GHz MMW exposures employing beam sizes of differing areas, ranging from 0.46 to 2.07 m^2. Previous laboratory and field studies (e.g., Parker, Nelson, Beason, & Cook, 2008) have indicated that the speed of the repel response is dependent upon, not only the power density on the target, but also the amount of the target surface area that is illuminated by the MMW beam. That is, given an initially stationary biological target, as more of the target area is illuminated by the beam, the quicker becomes the repel response (i.e., the more quickly the target moves out of or away from the beam). However, the exact form of this function relating area illuminated to repel time is unclear. Two studies were conducted to better quantify this relationship. Experiment 1 examined the repel times of initially stationary human subjects in response to 95-GHz MMW exposures at each factorial combination of three power densities and five spot sizes (i.e., beam diameters).

Experiment 2 was designed to determine the degree to which the relationships between beam size and repel time established in Experiment 1 extrapolated to the case of moving (non-stationary) subjects. Thus, in Experiment 2, subjects were required to throw balls into a net while being targeted by a 95-GHz MMW beam. Exposures were conducted employing the same five beam sizes used in Experiment 1. Effectiveness was measured as the difference between a subject's performance during "actual" exposures when they were targeted by the 95-GHz system and that same subject's performance during "sham" exposures (i.e., when they were not targeted).

2.0 METHODS

Procedures for data collection and treatment of participants were reviewed and approved by the U.S. Air Force Research Laboratory (Wright-Patterson Air Force Base site) Institutional Review Board and the U.S. Surgeon General's Human and Animal Research Panel. All applicable rules and regulations were followed.

2.1 Subjects

Prospective human subjects were recruited from among Tri-Care beneficiaries: active-duty, reserve, or retired military personnel and their dependents. All subjects were at least 18 years of age. Some, but not all, subjects participated in more than one experiment. No incentives were provided to induce participation other than the knowledge that subjects were assisting the Department of Defense to field a non-lethal weapon. Table 1 summarizes, for each of the experiments, the number, gender, and age of subjects, separately for those subjects who completed the experiment to which they were assigned and for those who failed to complete the experiment to which they were assigned. The four subjects who withdrew did so due to unforeseen scheduling conflicts.

Table 1. Number (*n*), gender, and age of subjects, separately for subjects who completed their assigned experiment and for those who did not, for Experiments 1A, 1B, and 2.

	Completed study					Failed to complete study				
		Gender[a]		Age			Gender		Age	
Study	*n*	M	F	Mean	*SD*	*n*	M	F	Mean	*SD*
1A	3	3	0	32.0	5.7	3	1	2	42.3	13.0
1B	15	13	2	35.6	12.8	0	0	0	—	—
2	20	18	2	31.7	11.0	1	1	0	60.0	0.0

[a]M = male, F = female.

2.2 Facilities and Beam Characterization

All MMW exposures were conducted at Frustration Canyon (Kirtland Air Force Base, Albuquerque, NM) using the Active Denial System (ADS) 0+.

For a given fixed distance from antenna, the ADS does not have the capability to dynamically modify the diameter of its beam. Therefore, for the present studies, effective beam size was controlled by varying the distance of the system antenna to the target (subject), with shorter distances corresponding to smaller beam sizes. Characteristic of focused beam systems, once beyond the Fresnel maximum (the location of minimal beam diameter, approximately 400 m from the antenna), the beam radius expands as a function of range to antenna. Beam divergence is minimal due to the advanced technology of the antenna, but it does produce an expanding spot with distance. Thus, five test sites were selected for the present studies (400, 550, 750, 850, and 1100 m away from the transmitter) that corresponded to five different incident beam areas (0.46, 0.62, 0.90, 1.40, and 2.07 m^2) During testing for both Experiments 1 and 2, ADS beam parameters (size, accuracy, and peak beam power density) were periodically characterized and verified at each of the five test sites.

Characterization involved use of a carbon-impregnated Teflon® plate (alternately referred to as carbon-loaded Teflon, or CLT). CLT is a homogeneous suspension of carbon powder in Teflon (PolyTetraFluoroEthylene polymer). Prior laboratory and field work has demonstrated that the CLT surface heats at rates similar to skin; therefore, measurement of CLT surface temperature

distribution using infrared (IR) thermography allows estimation of the beam parameters and skin heating rates (Durney, Massoudi, & Iskander, 1986; Ross, Allen, Beason, & Johnson, 2008). IR thermography of the exposed CLT was accomplished with one of two IR cameras that were accurate to within 2% of absolute temperature across IR wavelengths from 7.5 to 13 microns (FLIR Systems, Inc., Models ThermaCAM S65 and A320G, Wilsonville, OR). The IR imagery was captured on a portable computer at 30 frames per second. Power density was calculated using an empirical model which relates the temperature profile of the exposed CLT (specifically, peak temperatures) to the peak power density of 95-GHz radiation absorbed by the CLT (Ross et al., 2008).

Ground bounce and other MMW interference effects due to the environment were eliminated at each of the five target distances by positioning side-lobe absorbers at appropriate locations between the target area and the system antenna. The absence of any significant interference effects was verified by CLT measurements.

2.3 Experiments 1A and 1B

Experiment 1 consisted of two sub-studies, Experiments 1A and 1B. During each of these two studies, subjects underwent a series of exposure "sessions." A given session typically consisted of two 95-GHz exposures at a prescribed combination of ADS power density and ADS beam (spot) size. During one of the two exposures the subject's back was illuminated with the center of the beam focused on the subject's spine midway between waist and neck. During the other exposure, the subject's front was illuminated with the center of the beam focused on the subject's sternum.[1] The order of the two exposures (front versus back) was counterbalanced across subjects. During each of the two exposures male subjects were stripped to the waist; female subjects wore a sports bra or similar apparel. Removal of clothing was necessary to facilitate recording of subject skin temperature using one of the same IR cameras employed for beam characterization (see Section 2.2, *Facilities and Beam Characterization*). Subjects were instructed to remain motionless in the beam until they felt that the heat sensation induced by the MMW energy reached a point of "intolerability" at which time they were to move laterally behind a 0.3 m wide x 2.4 m high x 0.02 m thick plywood barrier that was impervious to the MMW beam. A maximum possible duration was imposed by the system operator for each exposure. This maximum duration varied as a function of the power density employed for the exposure; that is, the lower the power density, the longer the maximum possible duration, such that the total MMW fluence was approximately equal to 12 J/cm^2 for exposures at all power densities. Due to a software limitation of the transmitter controller, the pre-set duration was required to be a whole number of seconds. Thus, the duration for a given trial was set to the greatest integer less than 12 / power density. This fluence at the target was such that it ensured (a) almost all subjects exited the beam before the maximum duration was reached, and (b) an adequate safety margin was maintained (i.e., minimal possibility of skin damage even if a subject was able to remain in the beam until the maximum duration was reached).

For both studies, subjects were assigned to cohorts ranging in size from 2 to 7 subjects. Ideally, subjects within a given cohort would receive their exposure sessions over a period of

[1] The choice of beam location for Experiment 1 was dictated in part by the desire to compare data in the present study with that collected during prior ADS studies that had employed a similar methodology (including shot location).

approximately five experimental days. All exposures at a given spot size (test site) were delivered before exposures at the next prescribed exposure spot size commenced, and so forth until exposures for all five spot sizes were delivered. The order in which power densities were delivered at each spot size was randomized such that, although the order of the power densities experienced for all subjects within a given cohort was the same, the order differed from cohort to cohort. In addition, spot size was randomized such that the order in which the five spot sizes were experienced varied for the different cohorts. However, it was not always possible to adhere to this ideal schedule. Occasionally, for example, a subject from a given cohort would "drop out" of his or her assigned cohort due to scheduling conflicts, and would receive the remainder of their exposures after later reassignment to a different cohort.

The two experiments, 1A and 1B, differed from one another only in the number of power densities employed for the five spot sizes. Specifically, the first of the two, 1A, may be considered a pilot study involving $n = 3$ subjects (see Table 2). For each of the five spot sizes, Experiment 1A subjects were exposed to six different power levels (one front and one back exposure at each power density setting) for a total of 60 exposures per subject (5 spot sizes x 6 power densities x 2 orientations [front and back]). Based on analysis of the Experiment 1A subject data, a subset of three of the six power densities employed were chosen for use with the $n = 15$ Experiment 1B subjects. Thus, the Experiment 1B subjects received a total of 30 exposures over the course of the study (5 spot sizes x 3 power densities x 2 orientations [front and back]).

The six power densities used for Experiment 1A (1.6, 1.85, 2.1, 2.4, 2.7, and 3.0 W/cm^2) were chosen based upon the requirements that (a) the levels chosen be operationally relevant; (b) the differences between adjacent power density settings accord with the known resolution of the ADS system power settings; and (c) each setting be achievable at each (or at most) of the test sites (spot sizes) used in the studies. The minimum power density setting considered to be operationally relevant was established as 1.6 W/cm^2; the maximum was established as 3.0 W/cm^2. The minimum change in the System 0+ power density output on target that was achievable on a consistent basis was determined to be 0.25 W/cm^2. Thus, this constrained the smallest possible difference between adjacent power density levels. At the two sites furthest from the antenna (corresponding to the two largest spot sizes), the system was incapable of achieving a power density of 3.0 W/cm^2; thus, for these two sites, the power densities employed differed from those used at the closest three sites. Table 2 summarizes the power densities employed at each of the five spot sizes (sites) for both Experiments 1A and 1B.

Table 2. Power densities used for subject exposures at the five sites (coded A-E) — which correspond to the five spot sizes (0.46 – 2.07 m^2) — employed during Experiments 1A and 1B. Experiment 1B employed only those enumerated power densities displayed upon a yellow background. Experiment 1A used all of the enumerated power densities.

Site Code[1]				
A	B	C	D	E
Distance From ADS Antenna (m)				
400	550	750	850	1100
Spot Size[2] (m^2)				
0.46	0.62	0.90	1.40	2.07
Power Density (W/cm^2)				
1.60	1.60	1.60	1.60	1.60
1.85	1.85	1.85[a]	1.85	1.85
2.10	2.10	2.10	2.10	2.10
2.40	2.40	2.40	2.40	--
2.70	2.70	2.70	2.70	--
3.00	3.00	3.00	--	--

[1]Site A was nearest the ADS antenna at a distance of 400 m (viz., near the Fresnel maximum); Site E was furthest at a distance of 1100 m.

[2]The spot size for Site A was 0.46 m^2, for Site B was 0.62 m^2, etc. Note that all references to beam or spot size in this report, unless stated otherwise, refer to full width-half maximum (FWHM) of the major and minor axes of the two-dimensional Gaussian temperature distribution on the CLT surface.

[a]High winds (creating unsafe conditions) on the last scheduled day of testing for Experiment 1A precluded measurements at Site C for this combination of power density and spot size. Thus, Experiment 1A subjects received only 58 rather than the originally intended 60 total exposures. See Experiment 1 results for further details.

Subjects were examined at the conclusion of each exposure by a designated medical observer. Observers ensured that any skin redness (or any other heating effect) had resolved before a subject was permitted to participate in a subsequent exposure.

Dependent measures recorded for each exposure included repel time (i.e., the elapsed time from the start of the exposure until the subject initiated movement laterally away from the beam center and towards the protective plywood barrier), and subject skin temperature during the period immediately prior to and during the exposure. The measurements were derived from the IR videos collected during each trial.

2.4 Experiment 2

For Experiment 2, each of the n = 20 subjects (see also Table 1) was given a bucket of 30 tennis balls and instructed to throw as many of the balls as possible during a 30-s period into a designated target. The 30-s period of time defined a single trial. The target was a netted backstop container, constructed from PVC pipe and netting, measured 1.5 m high x 0.9 m wide x 1.2 m deep (see Figure 1). The target was located 7.6 m in front of the subject and approximately 20° degrees to the left or right of the ADS beam path. The positioning of the target to either the left or right of the beam was dependent on obstructions at a particular test site. The target was positioned off-

axis in order to avoid diffraction effects. A 0.3 m wide x 2.4 m high x 0.02 m thick plywood barrier, impervious to the 95-GHz beam, was situated approximately 1.6 m to the left of the center of the subject throwing location. The subject throwing location consisted of a rectangular area (demarcated by bright orange spray paint on the ground) measuring 0.9 m x 1.5 m. The subjects were instructed that quantity of balls thrown was more important than accuracy. (By way of example, it would be better to throw 20 balls into the target, missing with the other 10 [accuracy = 20 / 30 = 0.67] than to throw only 10 balls, but have all 10 end up in the target [accuracy = 10 / 10 = 1.00]. In the former [preferred] case accuracy is lower, but the number of balls on target is higher.) Any manner of throwing or moving was deemed acceptable so long as (a) only one ball at a time was thrown, and (b) both feet were within the 0.9 m x 1.5 m throwing area at the moment a given ball was thrown at the target. Balls landing in the target, but not thrown in accordance with these restrictions, were not counted as being on target.

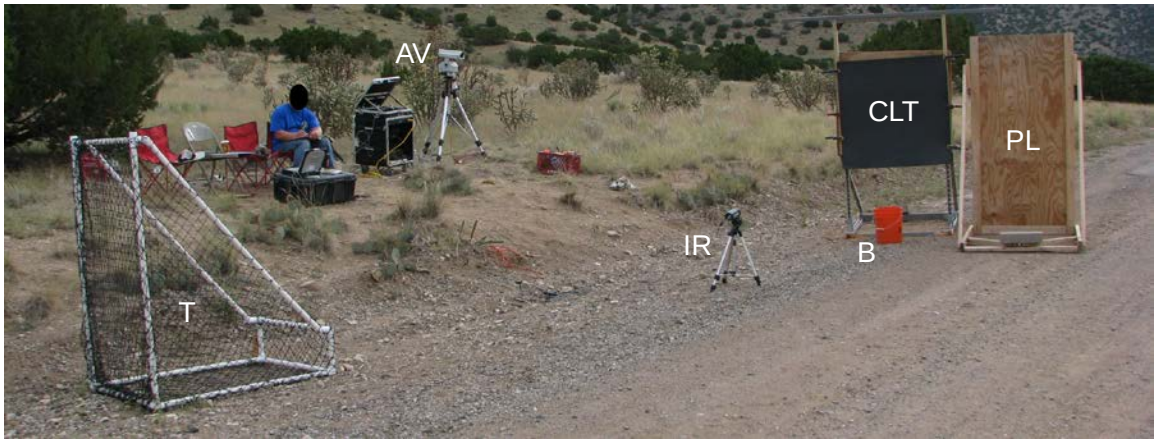

Figure 1. Set-up for Experiment 2. CLT = carbon-loaded Teflon (used for beam characterization), B = bucket of balls, PL = plywood barrier behind which subjects could move, T = target, IR = infrared camera, AV = audiovisual suite used to record subject behavior. During beam characterization, the carbon-loaded Teflon stand is situated where the subject throws balls (as in this figure), but is moved during the subject trials.

Subjects performed this task at each of the same five test sites (spot sizes) used in Experiments 1A and 1B. Subjects received four 30-s trials at each of the five sites for a total of 20 trials. As in Experiments 1A and 1B, subjects were assigned to cohorts ranging in size from four to six subjects. Ideally, subjects within a given cohort would receive their trials over a period of approximately five experimental days. All four trials at a given spot size (test site) were delivered before exposures at the next prescribed spot size commenced, and so forth until trials for all five spot sizes were delivered. A single, fixed power density was employed at each of the five test sites, this level being determined by the results of Experiments 1A and 1B. More specifically, the power density employed for Sites A-D was 1.85 W/cm^2; the power density used at Site E was 1.6 W/cm^2. (See Section 3.2.1, *Behavioral (Repel) Data*, for additional discussion on the rationale for selection of these power densities.) Spot size was randomized such that the order in which the five spot sizes were experienced varied for the different cohorts. As described above for Experiments 1A and 1B, it was not always possible to adhere to this ideal schedule.

For two of the four trials delivered for a given spot size, the subject was targeted by the 95-GHz SG transmitter operator. The subject was not targeted during the remaining two "sham" trials. Order of the trial type (actual exposure vs. sham exposure) was counterbalanced across

subjects. Subjects were not told before a given trial whether it was to be an actual exposure or a sham exposure, nor did they know how many sham exposures were planned for a trial. Subjects were informed that if they found themselves targeted by the ADS transmitter during a trial, and if the resulting sensation reached the point of intolerability, they should move laterally behind the adjacent plywood barrier. Subjects were free to remain behind the barrier for as long as they deemed necessary; they were similarly free to move back into the throwing area and resume throwing balls at the target (providing that the trial had not already concluded while they had been behind the barrier).

The timing of the MMW exposures during the two 30-s exposure trials was controlled by the ADS operator. The operator targeted the subject's center-of-mass (chosen in order to be consistent with the Experiment 1 targeting results, to maximize the probability of hitting the target, and to minimize the possibility of ground bounce effects). The operator would attempt to engage the subject at the commencement of an exposure trial. For a given power density, the operator was limited to shots of a maximum duration that ranged from 4 to 6 s. Following a given shot, a delay of 2 s was imposed before a succeeding shot could be taken by the operator. The operator was free to fire as many shots as possible during the 30-s trial as long as the fixed-length delay was maintained. The durations for both shot length and ensuing delay were based upon estimates from a thermodynamic model that computes the residual heat on human skin generated from multiple MMW exposures and were considered necessary for research purposes to reduce the risk of thermal injury.

Subjects were examined at the conclusion of each exposure trial by a designated medical observer. Observers ensured that any skin redness (or any other heating effect) had resolved before a subject was permitted to participate in a subsequent trial.

Subject behavior in Experiment 2 was captured using an audiovisual suite that included two digital video cameras (Pelco, Clovis, CA, M/N CC3751H-2) and two HD-DVD recorders (Panasonic, M/N's DMR-ES10 and DMR-T3040, Secaucus, NJ). One of the two cameras was situated relatively close to the subject (approximately 4-7 m) while the other was positioned near the target at which the subject was aiming. Dependent measures recorded for each trial included total number of balls thrown and number of balls on target.

3.0 RESULTS

3.1 Beam Characterization

Data collected during beam characterization indicated a beam profile that was elliptical.[2] Figure 2 depicts a typical IR image of the beam profile on a CLT sheet. Due to the geometry of Frustration Canyon, the occasional presence of dense flora between antenna and test site, and the size of the beam, the complete elimination of interference and/or diffraction effects was only rarely achievable. (Interference effects can be seen in the cross-hatch marks visible in Figure 2.) Sites

[2] It should be noted that the beam characterization procedures did detect sidelobes. However, these sidelobes were sufficiently separated from the main beam such that they did not hit the subject. Hence, this report refers to the distribution of MMW energy emitted by the ADS transmitter as approximately Gaussian with respect to the main beam axis.

were chosen that minimized these effects. (See also Section 2.2, *Facilities and Beam Characterization*, regarding the placement of barriers to further reduce interference effects.) Interference effects at the target location were considered to be sufficiently reduced when the difference between adjacent peak and tough temperatures throughout the CLT sheet was less than 1° C.

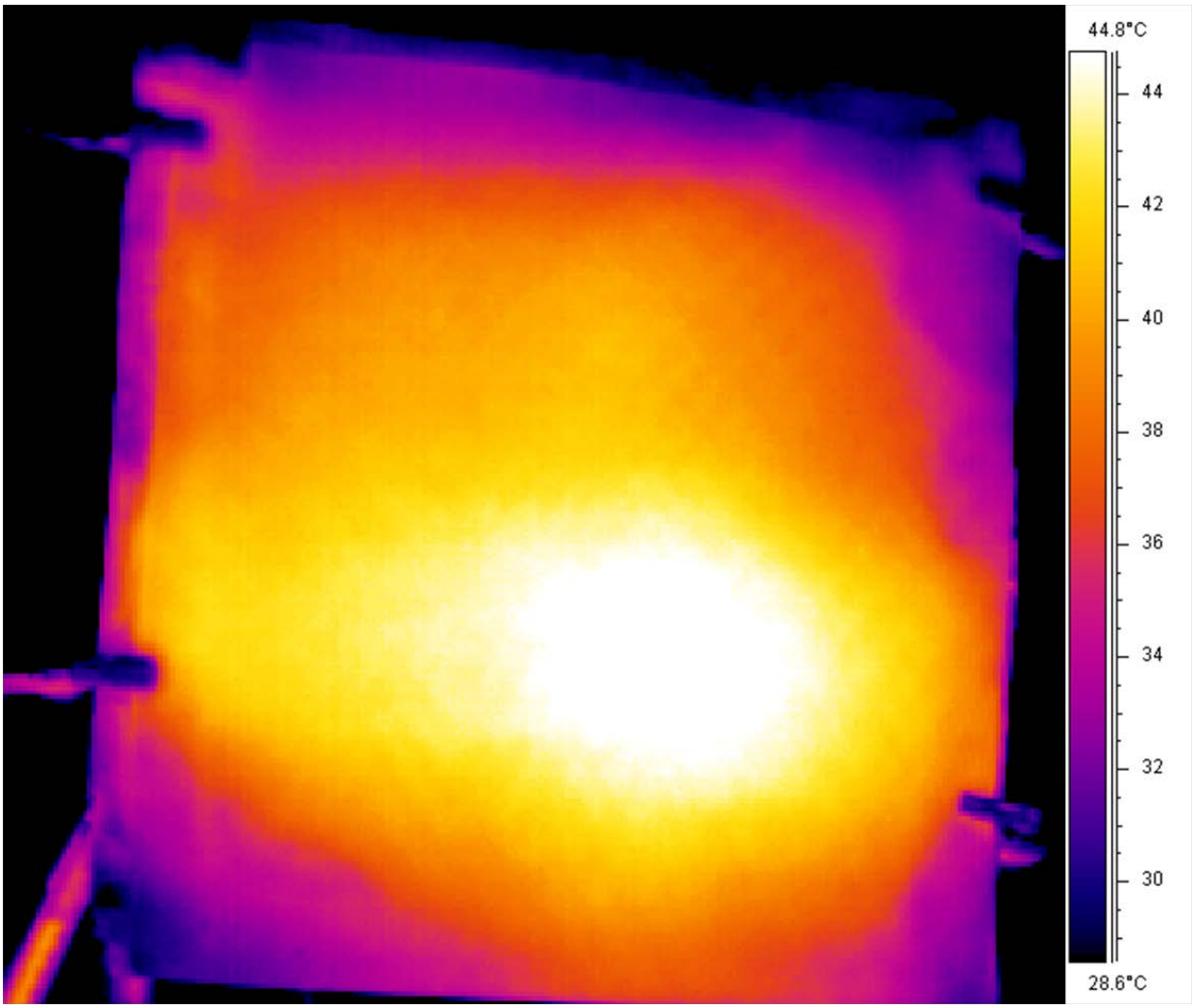

Figure 2. Representative infrared image of the Active Denial System 0+ beam profile on a 4 foot by 4 foot carbon-loaded Teflon plate. (Teflon surface temperatures increase as one moves from the plate periphery to its center. For this exposure [image] the change in absolute temperature from the edge of the CLT to the center of the spot is 13.5 °C.)

Variation in the measured spot size diameter at any given distance from the antenna was generally 5-10% of the mean value with the exception of the furthest distance. For the furthest distance, the spot size was as large as the CLT sheet and therefore more difficult to measure; thus, for this distance (spot size) the measurement variation was 20%. The Figure 3 scatter plot depicts the FWHM spot diameter for the beam's major and minor axes at different distances from the transmitter antenna (ranging from near the Fresnel maximum — approximately 400 m from the

antenna — to a point 1100 m from the antenna). The eccentricity of the elliptical beam (ratio of minor to major axis) when averaged over all exposures was 0.6. Figure 4 displays the FWHM spot area as a function of distance to the antenna where the area of the ellipse (spot) is defined as:

$$\text{area} = \pi/4 \times \text{FWHM major axis diameter} \times \text{FWHM minor axis diameter.} \quad (1)$$

Over the measured range, spot size area increases by a factor of approximately four.

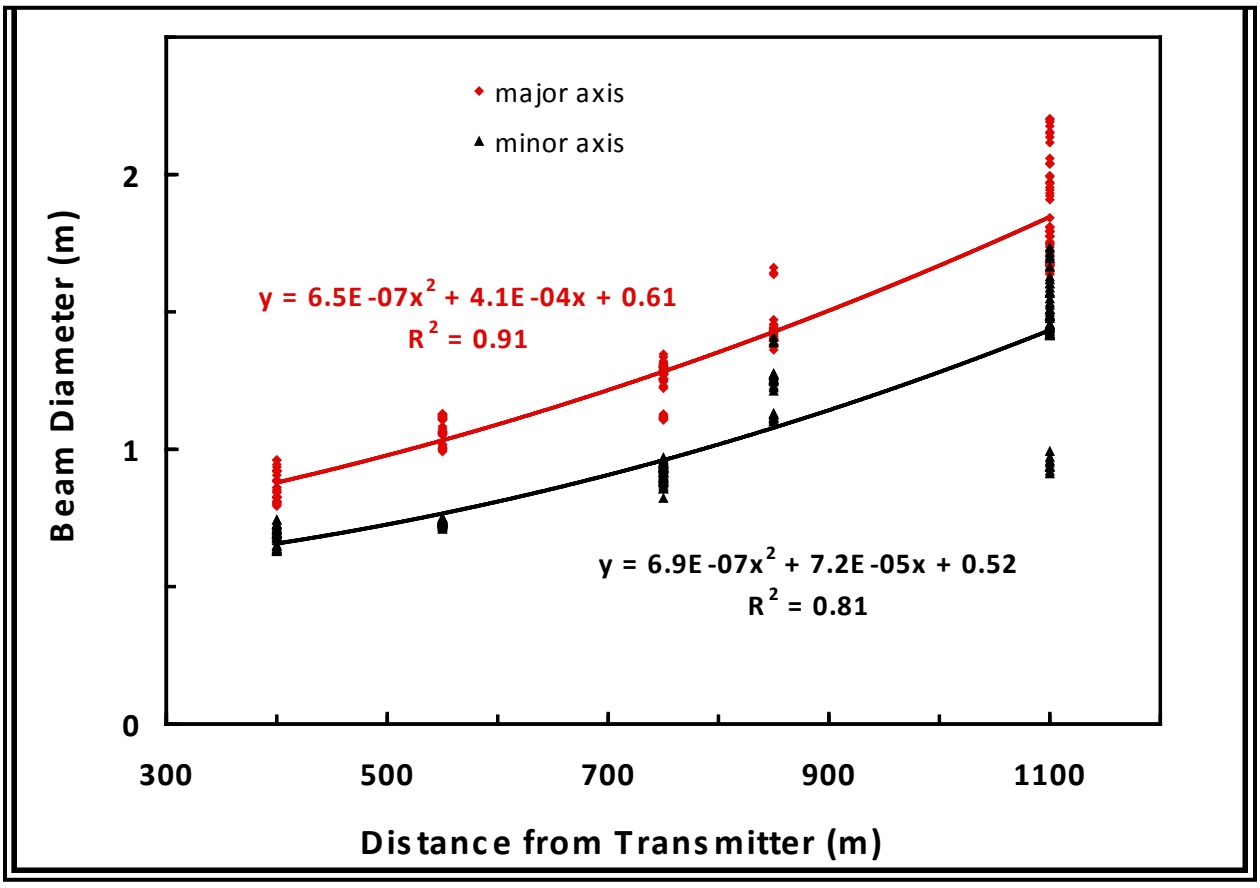

Figure 3. Variation in the diameter of the Active Denial System full width-half maximum spot (both major and minor axes) as a function of distance from the transmitter antenna. Distances at which measurements were obtained correspond to the five test sites used in Experiments 1 and 2. Equations presented are for the best-fit quadratic curves for the major (red) and minor axis data.

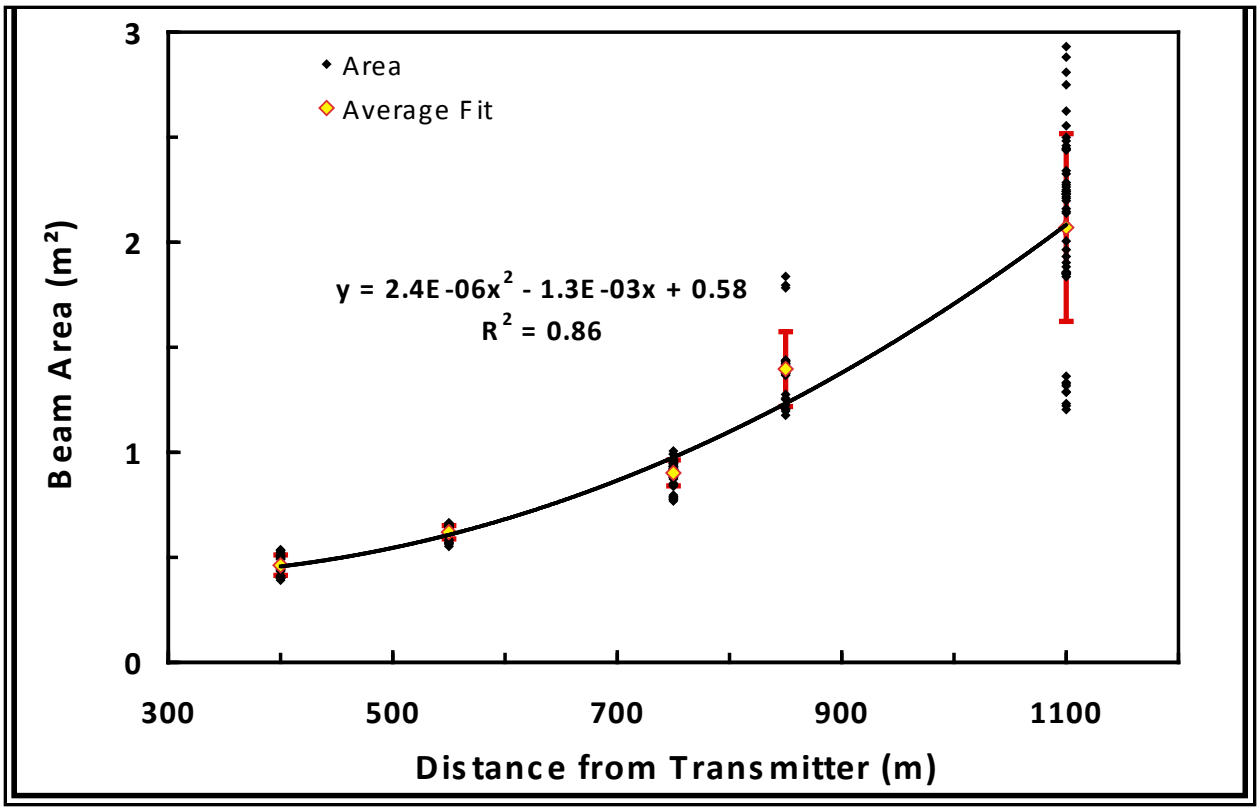

Figure 4. Variation in the area of the Active Denial System full width-half maximum spot as a function of distance from the transmitter antenna. Black dots = individual measurements; yellow diamonds = mean of the measurements at a given distance (± standard deviation). Distances at which measurements were obtained correspond to the five test sites used in Experiments 1 and 2. Equations are for the best-fit quadratic curve for the individual measurements.

Figure 5 depicts the variability found in ADS 0+ power density at each of the five test sites (spot sizes) employed in Experiments 1 and 2 during beam characterization measurements taken before and after subject exposures. For each test site, the figure summarizes the variation for the three power density levels utilized in Experiment 1B. As previously noted, these three power density settings (low, middle, and high) were not the same for the five sites. The precise targeted power density levels for each site are summarized in Table 2. The variability in the measured power density at each site/power density level combination represents the resolution of the device output. Throughout the three experiments the maximum standard deviation calculated for a given exposure condition was 0.23 W/cm^2, which corresponded to Site A (distance of 400 m) with power density set to 3.0 W/cm^2. The standard deviation of the combined data (all sites, all power density levels) was 0.07 W/cm^2.

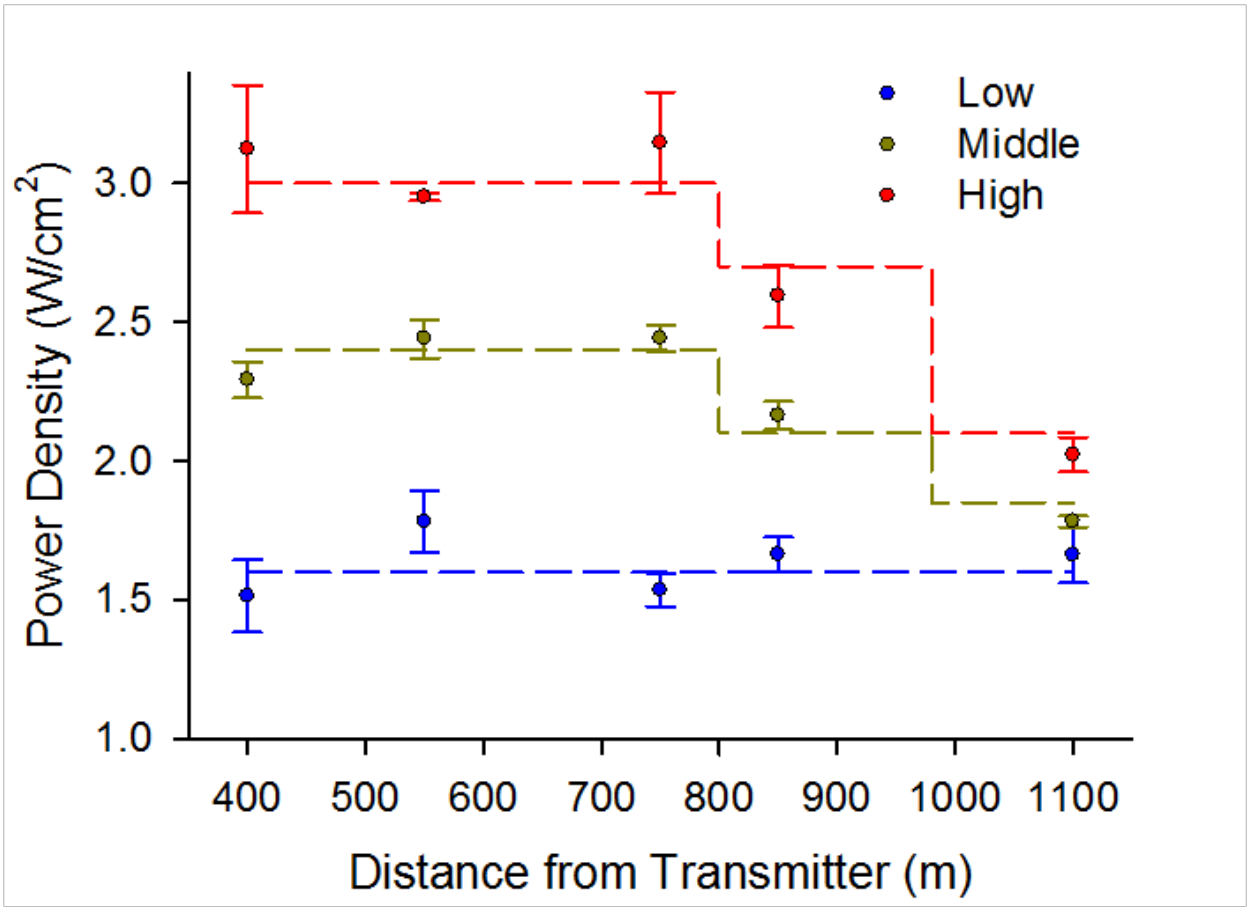

Figure 5. Variation in Active Denial System power density measurements (mean ± standard deviation) for the three different power density settings (low, middle, high) used in Experiment 1B as a function of distance from the transmitter antenna. Distances at which measurements were obtained correspond to the five test sites used in Experiments 1 and 2. Dashed lines indicate the desired low, middle, and high power density level on target that the system operator sought to achieve for each test site.

3.2 Experiments 1A and 1B

3.2.1 Behavioral (Repel) Data

Examination of the Experiment 1A repel data at the six power densities for each of the five spot sizes led to the selection of a subset of those power densities for use in Experiment 1B. Since the Experiment 1A results verified that each of the six power densities was effective in repelling subjects within an operationally relevant time frame, which was less than three seconds, a subset of power densities was chosen for Experiment 1B that maximized the range of power densities over which to test the subjects. Thus, for each of the five spot sizes, the maximum and minimum powers used in Experiment 1A were also used in Experiment 1B. For each spot size, the third power density used was simply the median power level that had been employed in Experiment 1A. The power densities chosen for Experiment 1B are summarized in Table 2. Because of the small number of subjects employed for Experiment 1A, detailed statistical analyses were not performed.

For Experiment 1B, the elapsed time to repel dependent measure was analyzed by a 2 (Exposure Orientation: front vs. back) x 3 (Power Density: low, middle, high) x 5 (Spot Size) repeated-measures analysis of variance (ANOVA). The analysis revealed a significant main effect for power density, $F(2, 28) = 36.44$, $p = 1.61 \times 10^{-8}$, $\eta^2 = 0.72$, reflecting a trend for higher power densities to result in quicker repel times. A marginally significant main effect for exposure orientation was uncovered, $F(1, 14) = 3.34$, $p = .09$, $\eta^2 = 0.19$, reflecting the tendency for frontal exposures to result in slightly faster repel times than corresponding back exposures employing the same exposure parameters (mean difference = 0.10 s).[3] Finally, the ANOVA revealed a significant Power Density x Spot Size interaction, $F(8, 112) = 9.63$, $p = 4.44 \times 10^{-10}$, $\eta^2 = 0.41$. Figure 6 depicts the form of this interaction. Planned comparisons — specifically, Bonferroni-corrected *t* tests — were used to contrast performance during exposures at the three power densities, separately for each of the five spot sizes. As can be seen from an inspection of Figure 6, for the two higher power densities (middle and high), repel times were relatively quick and tended to remain constant across the five spot sizes. However, at the lowest of the power densities, repel time was clearly impacted by spot size. For the largest spot size, the repel time at the low power density was equivalent to that found at the middle and high densities; however, as spot size decreased, repel times increased.

[3]Because neither main nor interaction effects involving exposure orientation achieved statistical significance, all subsequent analyses collapsed over this front versus back distinction.

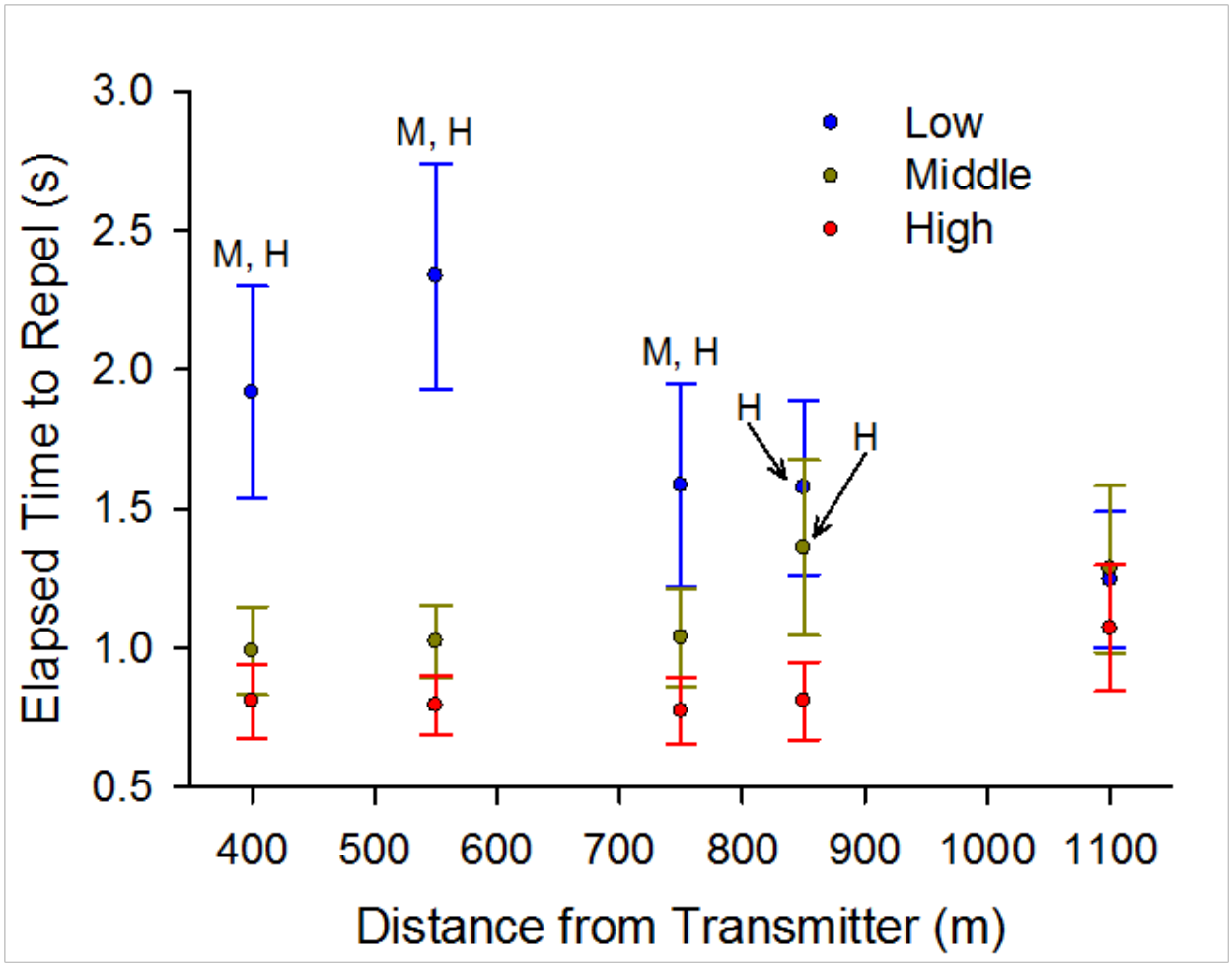

Figure 6. Mean elapsed time to repel (± standard error of the mean) for Experiment 1B exposures at three different power density settings (low, middle, high) as a function of distance from the transmitter antenna. M = the mean value near which the symbol is located differs significantly from the corresponding mean (i.e., at the same distance from the transmitter) for the middle power exposures; H = the mean value near which the symbol is located differs significantly from the corresponding mean (i.e., at the same distance from the transmitter) for the high power exposures.

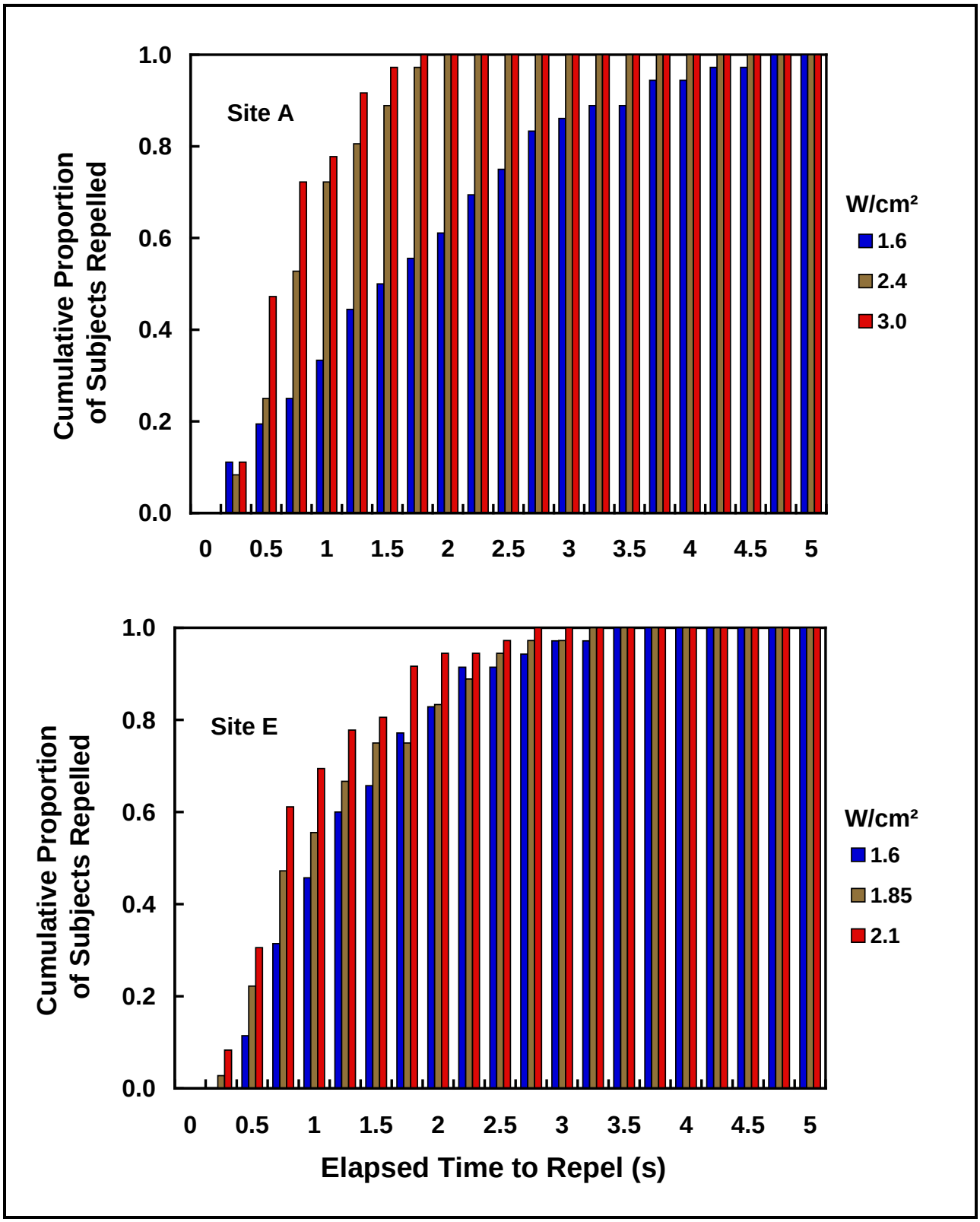

Figure 7. Cumulative proportion of Experiment 1B subjects repelled by the Active Denial System beam as a function of time to repel at three powers densities, separately for Site A (upper panel) and E (lower panel).

Figure 7 presents the cumulative histograms for subject repel data obtained at Sites A and E (which correspond to smallest and the largest spot sizes, respectively; see Table 2). The figure depicts an alternative method for representing and thinking about how spot size impacted subject performance during this study. Specifically, the figure shows the cumulative proportion of subjects who had been repelled by the ADS beam as the beam duration increased, separately for the three different power densities employed (1.6, 2.4 and 3.0 W/cm^2 at Site A, and 1.6, 1.85, and 2.1 W/cm^2 at Site E). An examination of the Site A data (upper panel) indicates that a beam duration of approximately 4.75 s was sufficient to repel all of the subjects exposed at the low power density (1.6 W/cm^2). However, as one might expect, this 100% threshold (i.e., cumulative proportion = 1.0) was met more quickly at the two higher power densities — for the 2.4 and 3.0 W/cm^2 exposures, 100% of the subjects were repelled given a beam duration of approximately 2.0 s. The Site A data shown in Figure 7 is representative also of the data for Sites B, C, and D in that the 100% repel threshold is attained more quickly for exposures at one or both of the higher power densities. This is not the situation, however, for Site E (lower panel), where the threshold is approximately the same for all three power densities. It may be the case that the different pattern of results at Site E relative to A-D is a function, not of the difference in spot size, but rather of the fact that — due to transmitter limitations — the difference between the lowest and highest powers at Site E (2.1 - 1.6 = 0.5 W/cm^2) was less than that for the other four sites (Sites A-C: 3.0 - 1.6 = 1.4 W/cm^2, and Site D: 2.7 -1.6 = 1.1 W/cm^2).

Figure 8 shows the data indicating the power density and spot size necessary to repel 90% of the subjects out of the ADS beam along with the corresponding repel times associated with that 90% threshold. The 90% threshold was calculated by determining the best fit Gaussian distribution for the exposure data for each combination of spot size and power density, and then estimating the repel time corresponding to the 90th percentile of the fitted Gaussian.

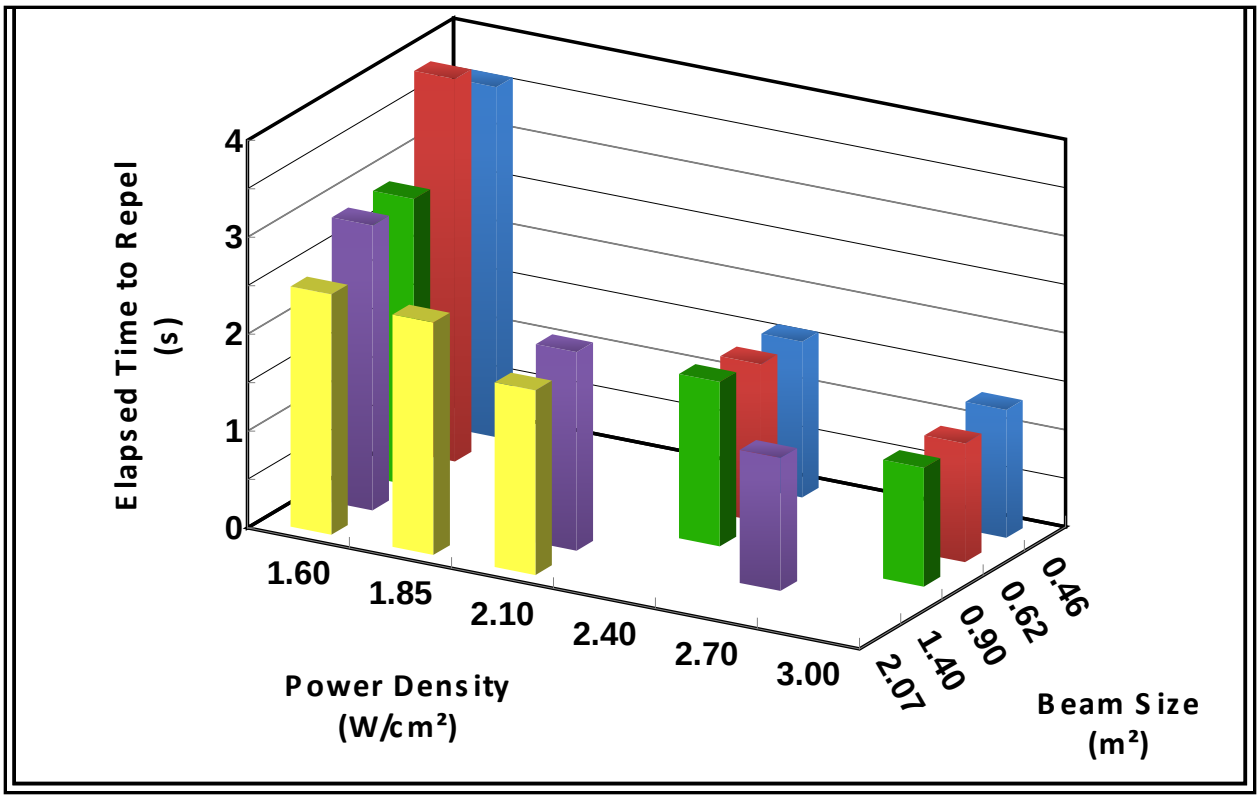

Figure 8. Elapsed time to repel 90% of subjects from the Active Denial System beam at each of the power density-spot size combinations used in Experiment 1.

Figure 9 depicts the effect of spot size on the threshold to repel 90% of the subject population over the range of spot sizes utilized in Experiment 1. Note once again that not all test sites (spot sizes) employed the same power densities (cf. Table 2). The data indicate a trend whereby as the spot size increases at given power density, there is a corresponding decrease in the time to repel until a threshold spot size is reached after which a plateau is achieved and further spot size increases do not change repel time. This trend is primarily evident at 1.6 W/cm^2, with indications of a bend in the relationship between spot size and repel time at a spot size of approximately 0.90 m^2.

Figure 9 also incorporates data from Raytheon Company's Silent Guardian™ (SG) system, a 95-GHz exposure system constructed along principles similar to that of the ADS but with a smaller spot size (Parker et al., 2008). The Figure 9 SG data point represents the mean of a series of exposures at a power density of approximately 3.0 W/cm^2. Comparing this data point average with the Experiment 1 exposures at 3.0 W/cm^2 appears to show that the "threshold" spot size (i.e., where the point where changes in spot size begins to impact repel) moves towards the left as the power is increased. Thus, there is a relationship between power density and spot size, but it is not a linear one. The data at 2.4 W/cm^2 seem to refute this trend, but the variance in those data (not shown in the figure) is so large as to preclude any statistically definitive statements regarding the hypothesized trend. Because the threshold (or bend) moves towards the left as the power density increases, the required power level for a given repel time varies less as the spot size increases, and appears to eventually "plateau" or cease to depend upon spot size.

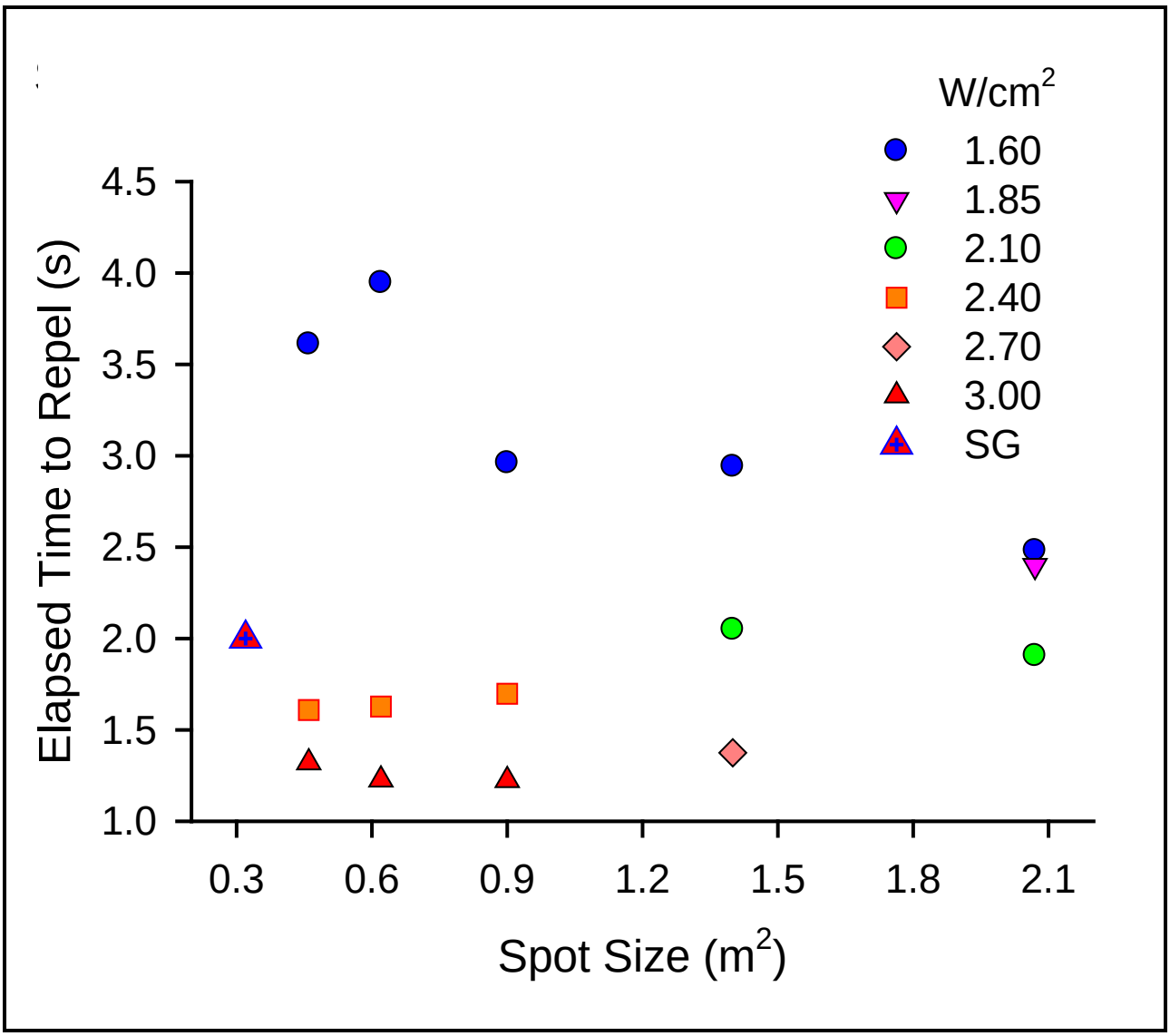

Figure 9. Elapsed time to repel 90% of subjects at each of the power density-spot size combinations used in Experiment 1 from the Active Denial System beam and from the Raytheon Silent Guardian (SG) system beam.

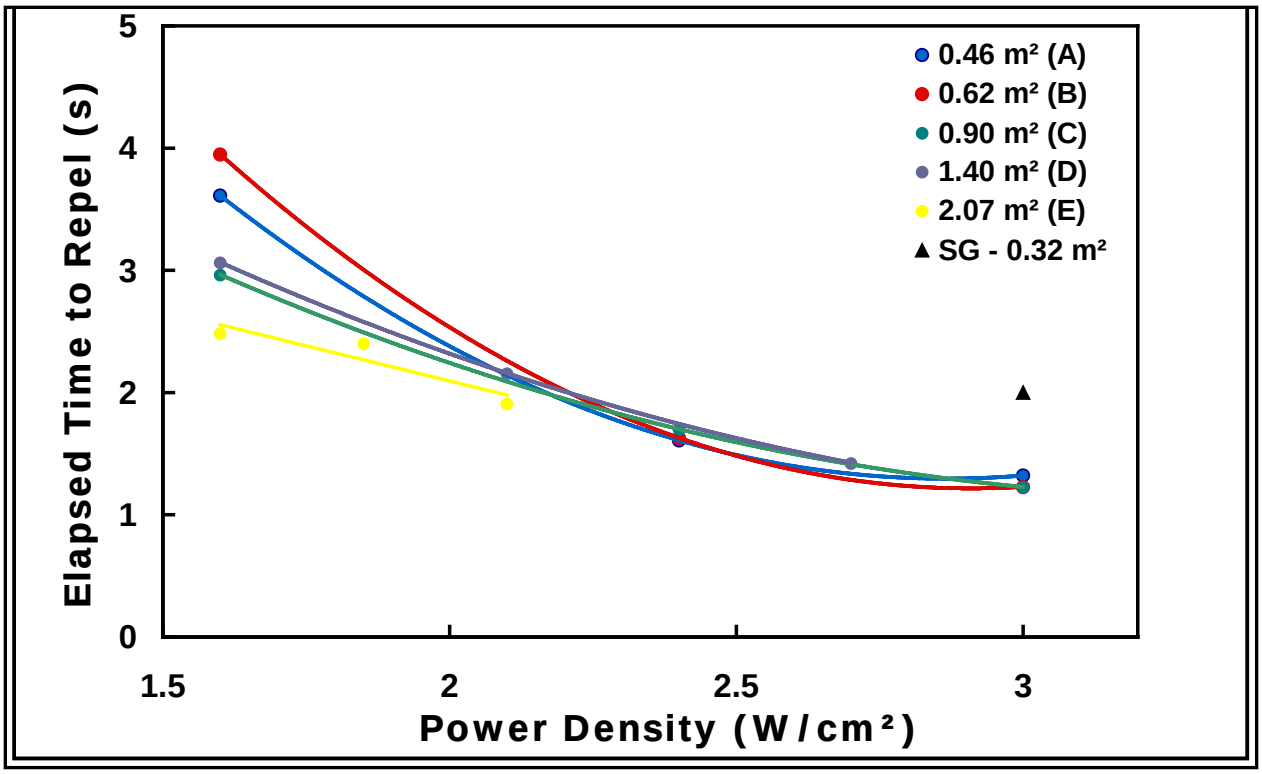

Figure 10. Elapsed time to repel 90% of subjects at each of the power density-spot size combinations used in Experiment 1 from the Active Denial System beam and from the Raytheon Silent Guardian (SG) system beam. For spot sizes 0.46, 0.62, 0.90, and 1.40 m^2, the trend lines are quadratic functions of best fit; for the 2.07 m^2 spot size, the trend line is a linear function of best fit. The horizontal line represents a constant repel level (2.5 s) across all spot sizes and was used to determine the Experiment 2 power densities.

Figure 10 depicts the same relationship as does Figure 9, but in this instance power density (as opposed to spot size) appears on the horizontal axis and the individual trends represented are for each of the different spot sizes across those power densities. As in Figure 9, Figure 10 also includes the data point for the SG repel response. The figure also shows quadratic functions of best fit for the spot sizes 0.46, 0.62, 0.90, and 1.40 m^2 (Sites A-D). A linear function is fit to the data for the 2.07 m^2 spot size (Site E). Examination of the best fit lines highlight the trend towards equivalent repel times as power density gets sufficiently high independent of spot size for the range of spot sizes used in Experiment 1. The repel response to the SG system indicates that there are still spot size dependencies out to 3.0 W/cm^2 if the spot is small enough. As the repel effect is believed to be mediated by nerve fiber summation, the more nerve fibers activated, the stronger the response. Apparently once a large enough section of the body is heated *at sufficient intensity*, the response no longer depends upon spot size.

The selection of power densities to use at each of the five spot sizes for Experiment 2 was guided by the desire to choose values that would result in a constant behavioral effect at each spot size. Referring to the Experiment 1 repel data summarized in Figure 10 highlights how this was done. Since the repel response variation across spot size becomes more pronounced as repel time increases, we chose to use the longest repel time that was measured across all sites (see the horizontal line in Figure 10), which turned out to be approximately 2.5 s. The intersection of this

horizontal line with the best-fit trend lines determined the power densities to be used in Experiment 2 for each spot size. Examining the figure, those powers should be: Site A = 1.97 W/cm^2, B = 2.02 W/cm^2, C = 1.85 W/cm^2, D = 1.90 W/cm^2, and E = 1.6 W/cm^2. However, since the power resolution of the transmitter was only 0.25 W/cm^2 and the range of powers required for Sites A-D was only 2.02 – 1.85 = 0.17 W/cm^2, a single power density of 1.85 W/cm^2 was chosen for Sites A - D. Site E used 1.6 W/cm^2 for the exposures in Experiment 2.

3.2.2 Medical Examinations

The Experiment 1A and 1B exposures resulted in a single blistering incident. Two small blisters (each less than 5 mm in diameter) formed on the subject's chin approximately 24 hr following exposure. No medical intervention was required for either of these small blisters.

3.3 Experiment 2

For Experiment 2, dependent measures (the number of balls that were accurately thrown [i.e., in the target area] during a 30-s trial and total number of balls thrown during a trial) were analyzed by separate 2 (Trial Type: actual exposure vs. sham exposure) x 2 (Trial Number: first vs. second trial) x 5 (Spot Size) repeated-measures ANOVAs. Both analyses revealed a significant main effect for trial type, $F(1, 19) = 78.44$, $p = 3.58 \times 10^{-8}$, $\eta^2 = 0.81$ for number of accurately thrown balls and $F(1, 19) = 105.35$, $p = 3.45 \times 10^{-9}$, $\eta^2 = 0.85$ for total number of balls thrown. That is, for both measures, performance was adversely impacted by exposure to MMWs. As expected, subjects performed better during sham than during the actual exposures. In addition, both analyses revealed a significant main effect for trial number, $F(1, 19) = 17.05$, $p = .00057$, $\eta^2 = 0.47$ for number of accurately thrown balls and $F(1, 19) = 53.25$, $p = 6.38 \times 10^{-7}$, $\eta^2 = 0.74$ for number of balls thrown. These effects highlight a practice effect, with subjects tending to perform better during Trial 2 than Trial 1 (collapsing over the sham vs. actual exposure factor).

Further, the analysis for number of accurately thrown balls uncovered a significant main effect for spot size, $F(4, 76) = 8.67$, $p = 8.12 \times 10^{-6}$, $\eta^2 = 0.31$. Finally, the analysis for total number of thrown balls resulted in a significant Trial Number x Spot Size interaction, $F(4, 76) = 3.75$, $p = .0077$, $\eta^2 = 0.16$. For each of the two dependent measures, planned comparisons were conducted to identify the locus of the significant effects. Specifically, Bonferroni-corrected *t* tests, contrasting performance across the five spot sizes separately for each factorial combination of trial type and trial number, were calculated when the relevant simple main effect was significant. Figure 11 illustrates these effects for the two dependent measures. In sum, these figures show an effect of beam size on performance. However, this effect is confined, as one would expect, to the exposure trials. For the exposure trials, contrasts reveal a modest improvement in subject performance that is confined to the smallest beam size, 0.46 m^2.

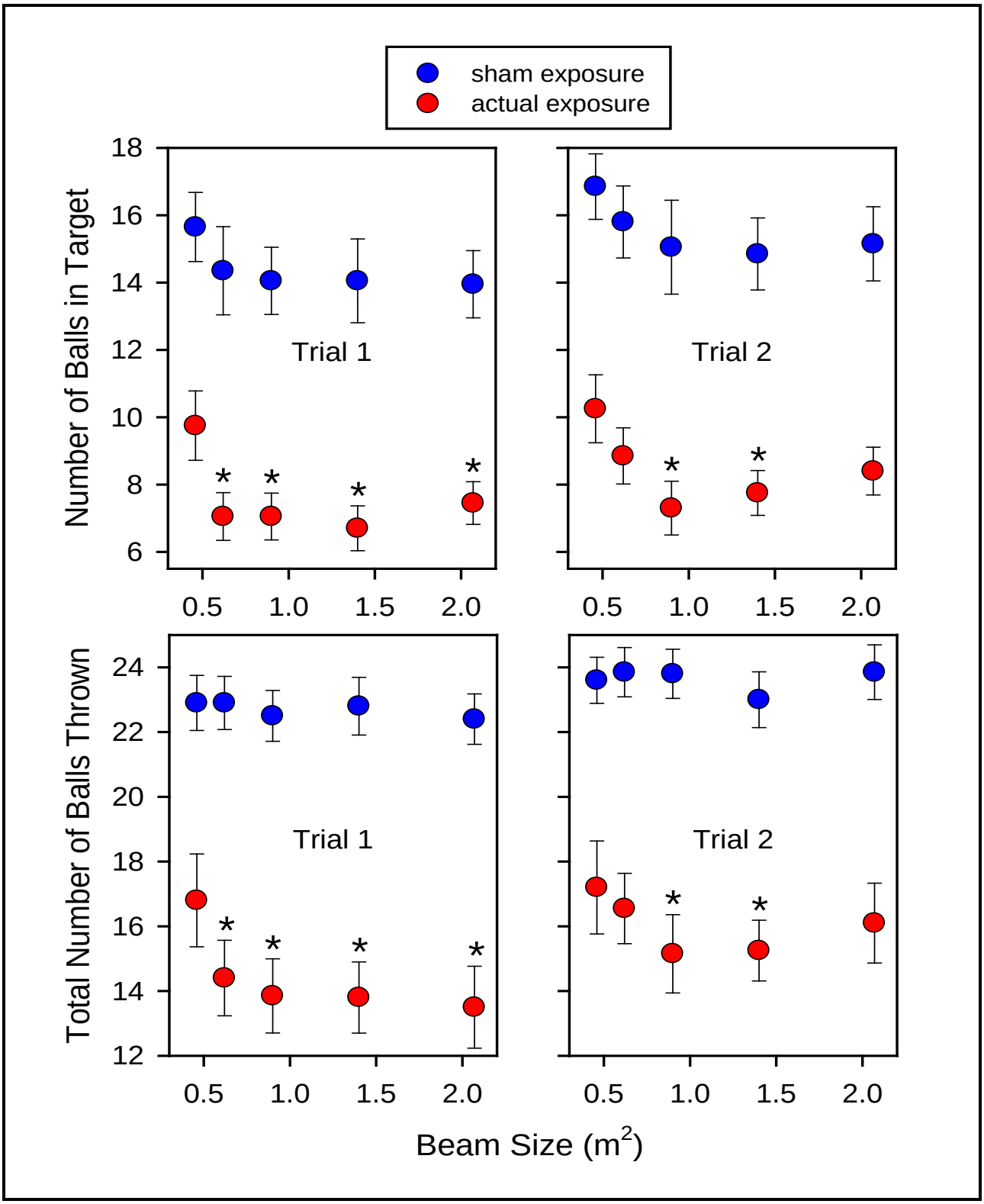

Figure 11. Number of balls thrown on target (upper panel) and total number of balls thrown (lower panel) (± standard error of the mean) by Experiment 2 subjects during actual exposure trials using each of five Active Denial System spot sizes, along with performance during corresponding sham exposure trials.

3.3.1 Medical Examinations

The Experiment 2 trials resulted in one incident of blistering. A small (less than 5 mm in diameter) blister was noted on the right bicep of a subject after the second of two exposure trials on that subject's final test day. No medical intervention was required for the blister. Although the bicep was not explicitly targeted during the trial, the operator was attempting to hit a moving target which caused multiple areas to be exposed.

4.0 CONCLUSIONS

4.1 Sufficiently Large Spots

The current understanding of the human repel response to exposures of sufficiently intense MMW energy indicates that responses of thermally sensitive nerve endings over the MMW-heated sections of the body are summed to generate an aversion signal that is processed at the reflexive response level (cf. Schmidt, Schmelz, Ringkamp, Handwerker, & Torebjork, 1997). This theory would indicate that with sufficiently large spots sizes, where all available nerves have been exposed, the repel response (or time to effect, TTE) must become independent of spot size. These plateaus in TTE were seen throughout the behavioral data for Experiment 1 (e.g., Figure 10), lending support for this hypothesis. For designers of MMW systems, this finding provides a bound upon the response that individuals will have that is related to the spot size of a proposed system.

Additionally, the threshold spot size at which a given power density becomes a constant function of spot size decreases with increasing power density. Thus, for 1.6 W/cm^2, TTE is nearly constant for spot sizes greater than 0.90 m^2; at 3.0 W/cm^2, however, the threshold spot size is about 0.46 m^2 (see Figure 9). The signal that mediates the repel response must be a function of both intensity of the stimulus and the number of nerves activated. Thus, the nerve summation effects are apparently saturated once a sufficiently large stimulus is generated. This again has implications for future MMW systems as it provides a trade space for beam size and power density available on target. Since the total power available and the antenna gain are design constraints of a MMW system, understanding the beam size and power density trade space will define the operationally effective ranges for the proposed design. Given the warfighter's requirements for a specific system, the designers can use the trade space information to optimize the system for a desired operational range with minimal power requirements.

4.2 Small Spot Trends

For a constant power density, the existing data indicate that as the spot size is reduced below a given threshold size, the TTE increases dramatically. The threshold spot size at which the TTE rise occurs is a function of power density (c.f. Section 3.2.1, *Behavioral (Repel) Data*, and Figure 9). Following the nerve summation hypothesis, this effect is explained by the condition that a faster repel response is proportional to the strength of the signal until a saturation condition is met. If the stimulus intensity is constant (by setting the power density to a constant), then the size of the repel signal is proportionate to the spot size. A large repel signal would correspond to a small TTE, and conversely the smaller signals to longer TTEs as observed in Figure 9. The precise relationship of TTE to spot size across all power densities of interest needs to be determined, but

at this time more data is necessary to make definitive statements regarding the functional form of that relationship.

4.3 Streamlines of Constant Power Density

By defining the relationship between spot size, power density, and TTE to be governed by a nerve summation effect, one can utilize potential theory to develop continuously deformable streamlines of constant power density that represent the relationship of spot size versus TTE. These streamlines would be parallel at sufficiently large spot sizes where additional sensory summation effects are no longer relevant in accordance with the description in Section 4.1, *Sufficiently Large Spots*, and would curve upwards at small spot sizes as described in Section 4.2, *Small Spot Trends*. The current data lends support to the development of these streamlines, but the data is too sparse to provide significant confidence intervals to any results. The issue is that the range of spot sizes over which this study was conducted was limited by the capability of the ADS 0+ to vary its spot size. This range of spots sizes had few data points in the region where the streamlines bend. Thus, the uncertainties in the best-fit trendlines are large enough that the functional form cannot be well defined.

4.4 50% Threshold Study

The uncertainties in the functional form of the streamlines could be reduced with additional data. There already exists a significant database of MMW effects, but most of it is confined to a few different spot sizes. Further, much of the existing data pertains to endpoints other than the 90% repel response defined in the present study. Of interest would be an investigation of 50% repel levels, as this would enable additional comparisons to be extracted from already existing reports.[4] For example, the data from the SG study generated only a single 90% point for TTE; however, by re-examining the data for the 50% thresholds, four additional data points could be generated relating TTE to power density at the SG spot size. In addition, research conducted at Brooks City-Base will provide information on responses at higher power and smaller spots. Finally, exposures at lower power densities could provide thresholds for pain intolerability, which would provide lower bounds to the potential function. Any future studies should involve improving the model development.

Utilizing a 50% as opposed to a 90% threshold does create a potential problem for actual weapon parameters. Rarely would one want to design a weapon that only works against 50% of its targets. In fact, since these thresholds are defined using static targets, the operational effectiveness (i.e., against moving targets) would presumably be less than the static threshold value. This has been the governing reason why most MMW experiments have focused on determining a 90% threshold — so that the weapon will still have a significant operational effect. However, the richer 50% threshold data set would provide a more reliable functional relationship for spot size, and thereby model development. By using existing data showing the increase in

[4]In the process of experimentally determining a 90% threshold, past data often started by determining 50% threshold. To ensure subject safety, MMW repel studies are often designed such that subjects are initially exposed at relatively low power densities that repel few, if any, subjects; power densities are then incrementally increased over successive exposures until a 90% threshold is attained. Thus, a study designed to detect a higher repel threshold (e.g., 90%) may by virtue of its methodology detect a lower one (e.g., 50%) as well.

power density required to move from a 50% to a 90% threshold at specific exposure conditions, conservative estimates could be generated that allow the conversion of the higher fidelity streamlines created with 50% repel estimates to more operationally relevant 90% threshold streamlines.

4.5 Need for Smaller Spot Study

As mentioned in Section 4.3, *Streamlines of Constant Power Density*, the current study was limited to investigating spot sizes greater than 0.46 m^2. However, that appears to be the upper threshold of a region where spot size effects become more pronounced. Comparisons of laboratory data (with spot sizes less than 0.07 m^2) to field data that employed the ADS indicated that spot size would affect the repel response, but the scarcity of data precluded an exact understanding of that relationship. Previous data from the SG study (cf. Parker et al., 2008) indicates a significant increase in TTE at 3.0 W/cm^2 and spot size = 0.32 m^2 compared to exposures in this study at the same power density but with larger spot sizes (see Figure 9). Although the data at 1.6 W/cm^2 also indicates a TTE dependence that is strictly due to spot size effects, the other data does not. This anomalous result is likely due to the fact that the region where the spot size effects are most dramatic was not investigated due to the inability of the existing MMW transmitters to generate the desired spots. To fully explore the region where spot size effects are more pronounced, an additional study is necessary that investigates spot sizes in the range of 0.07 to 0.46 m^2. Spot sizes below 0.07 m^2 have already been studied in the laboratory at Brooks City-Base. Once the full range of spot sizes has been investigated, optimal ADS designs may be generated from the collected data and improved models.

A study can be designed that explicitly defines the power densities of interest. Such a study might utilize the SG system. The beam characterization of the SG device (Parker et al., 2008) indicated that it is capable of generating spots in the range of 0.08 to 0.32 m^2 at operationally relevant power densities. Other MMW sources could be used for the suggested study; the SG device is proposed simply because there are no modifications necessary to enable it to produce the desired power densities and spot sizes.

REFERENCES

Durney, C. H., Massoudi, H., & Iskander, M. F. (1986). *Radiofrequency radiation dosimetry handbook* (4th ed.) (Rep. No. USAFSAM-TR-85-73). Brooks Air Force Base, TX: USAF School of Aerospace Medicine.

Erwin, D. N. & Hurt, W. D. (1981). *Assessment of possible hazards associated with applications of millimeter-wave systems* (Rep. No. Review 2-81). Brooks Air Force Base, TX: US Air Force School of Aerospace Medicine.

Gandhi, O. P. & Riazi, A. (1986). Absorption of millimeter waves by human beings and its biological implications. *IEEE Transactions on Microwave Theory and Techniques, 34,* 228-235.

Parker, J. E., Nelson, E. J., Beason, C. W., & Cook, M. C. (2008). *Thermal and behavioral effects of exposure to 30-kW, 95-GHz millimeter wave energy* (Rep. No. AFRL-RH-BR-TR-2008-0055). Brooks City-Base, TX: Air Force Research Laboratory.

Ross, J. A., Allen, S. J., Beason, C. W., & Johnson, L. R. (2008). Power density measurement of 94-GHz radiofrequency radiation using carbon loaded Teflon and infrared imagery. Unpublished manuscript.

Schmidt, R., Schmelz, M., Ringkamp, M., Handwerker, H. O., & Torebjork, H. E. (1997). Innervation territories of mechanically activated C nociceptor units in human skin. *Journal of Neurophysiology, 78,* 2641-2648.